JOURNAL OF OPTOELECTRONICS AND ADVANCED MATERIALS Vol. 9, No. 8, August 2007, p. 2560 - 2565

Sol-gel composing hybrid precursors to synthesize $REBO_3$: Ln^{3+} (RE = Y, Gd; Ln = Eu, Tb) submicrometer phosphors

BING YAN*, CHONG WANG
Department of Chemistry, Tongji University, Shanghai 200092, P. R. China

$REBO_3$ (RE = Y, Gd) submicrometer phosphors doped with different content of Eu^{3+} and Tb^{3+} were synthesized by a modified sol-gel technology. Through the sol-gel process of borate source (tri-n-butyl borate, abbreviated as TBB), rare earth coordination polymers of salicylate and polyethyl glycol (PEG) were in-situ assembled to hybrid precursors. After the thermal decomposition of these hybrid polymeric precursors, the solid phosphors can be obtained, whose microstructure and particle sizes may be controlled by the hybrid precursors. X-ray diffraction (XRD) indicates these phosphors present hexagonal phase with vaterite-type structure. Scanning electron microscopy (SEM) suggests they show uniform size with submicrometer grains of around 100 – 300 nm. The photoluminescent behavior of these phosphors with different Eu^{3+} and Tb^{3+} ions concentration (1, 3, 5, 7, 8 mol %, respectively) were studied in details. The orange to red emission intensities ratios exhibit different behavior for different host of YBO_3 and $GdBO_3$.

(Received April 17, 2007; accepted June 2, 2007)

Keywords: Sol-gel synthesis, Luminescence, Phosphors, $REBO_3$:Ln^{3+}

1. Introduction

Inorganic luminescent materials have considerable practical applications in almost any devices involving the artificial production of light. Cathode ray tubes, lamps and X-ray detectors are well-known examples [1]. In recent years, a great deal of interest has been focused on the fabrication and luminescence properties of a wide variety of oxide based phosphors in order to make flat panel displays more commercially viable [2-4]. (Y, Gd)BO_3 belongs to one of the best host of phosphors available for the red or green primary of the color picture in plasma display panels (PDPs) and possible use in Hg-free lamps [5]. A high-UV transparency added to an exceptional optical damage threshold allows them to withstand easily the harsh conditions present in vacuum during the gas discharge [6]. (Y, Gd)BO_3: Eu^{3+} phosphors were extensively studied in spite of their relatively low and luminescent efficiency and limited chromaticity for the practical applications in cathode radial tube (CRT) and fluorescent lamps [7-16]. In order to fulfill the requirement of good photoluminescence characteristic under the illumination of vacuum ultraviolet (VUV) photons, such as high luminescence efficiency, good chromaticity, chemical and environment stability and long lifetime, a great effort has been made to improve luminescence properties of YBO_3: Eu^{3+} by adding some other dopants such as Bi^{3+}, La^{3+} and Sc^{3+} etc [17]. Besides, other photoactive species can be doped in the Y(Gd)BO_3 host such as Tb^{3+}, etc, which can exhibit strong green luminescence [18-22].

Traditional synthesis methods of submicrometer luminescence materials were mainly focused on the solid state reaction, hydrothermal process and spray-pyrolysis, etc. Jagannathan *et al* [23] employed some organic polymers to serve both as fuel and dispersing medium for nanocrystal formation, which can limit the agglomeration of particles to some extent. In this paper, we selected salicylate coordination polymers and nitrate as the precursors of luminescent species, polyethyl glycol (PEG) as dispersing medium template, which were assembled with other functional component such as tri-n-butyl borate (TBB) for the precursor of the borate network and urea for a fuel. The submicrometer materials, $REBO_3$ doped with Eu^{3+} and Tb^{3+}, were synthesized by the thermolysis of the hybrid precursors at 1100 °C. The luminescence performance, structure and grain sizes were systematically examined.

2. Experimental

2.1 Chemicals and procedures

The starting materials RE_2O_3 (RE = Y, Gd, Eu) and Tb_4O_7 were firstly dissolved into concentrated nitric acids to convert to their nitrates. The synthesis of $REBO_3$: xLn^{3+} (RE = Y, Gd; Ln = Eu, Tb; x = 1, 3, 5, 7, 8 mol %, respectively) by rare earth salicylate coordination polymers-PEG precursors are described below: Excess salicylic acid (3.1 mmol) was dissolved in 95 % ethanol (10 ml solution) and its *p*H value was adjusted to be about 7.0 with ammonia solution, then rare earth nitrates with different concentrations were added and mixed homogenously. After that, urea, PEG and stoichiometric ammonia solution were added into the above solutions and heated under 60 °C by dipping diluted HNO$_3$ solution until the solution becomes acidic The heating temperature was increased to 100 °C to evaporate the solvent until the solution becomes viscous to form the gel. After drying the gel, then the precursors were obtained finally. It was worth to note that the thermal decomposition temperature was 1100 °C to remove the organic component in rare earth coordination polymeric systems. The typical scheme of the synthesis can be shown as below:

$$(1\text{-}y)\ Y(NO_3)_3 + y\ Gd(NO_3)_3 + x\ Eu(NO_3)_3$$

$$(Tb(NO_3)_3) + 3.1HSal + mNH_3{\cdot}H_2O$$

$$\longrightarrow [Y_{1\text{-}y}Gd_y(Sal)_3]_n + x\ [Eu(Tb)(Sal)_3]_n + TBB + nPEG$$

$$+ nNH_2\text{-}CO\text{-}NH_2 + mNH_3{\cdot}H_2O$$

$$\longrightarrow Y_{1\text{-}y}Tb_yBO_3\text{: } xEu^{3+}\ (Tb^{3+}) + CO_2\uparrow + H_2O\uparrow + NH_3\uparrow +$$

$$NO_2\uparrow$$

2.2 Physical measurements

The submicrometer particle was characterized by means of X-Ray diffraction (XRD, Bruke, D8-Advanced, CuKα target with a working voltage of 40kV and a current of 40 mA) and scanning electric microscope (SEM, Philps XL-30). Luminescence spectra were recorded with Perkin-Elmer LS-55 model fluorophotometer (scan rate = 1000 nm/s, excitation slit width = 10 nm, emission width = 5 nm).

3. Results and discussion

The X-ray powder diffraction patterns of REBO$_3$: Ln^{3+} calcined at 1100 °C for 3 hours are recognized that these phosphors belong to single phase. Fig. 1 shows the selected XRD profiles of YBO$_3$: 0.05Eu^{3+}, Y$_{0.5}$Gd$_{0.5}$BO$_3$: 0.05Eu^{3+}, Y$_{0.3}$Gd$_{0.7}$BO$_3$: 0.05Eu^{3+}, GdBO$_3$: 0.05Eu^{3+} and GdBO$_3$: 0.05Tb^{3+}, which are denoted with a, b, c, d, and e, respectively. Fig. 1 gives the XRD of five selected submicrometer phosphor samples, and it can be clearly observed that the submicrometer phosphors derived from the rare earth coordination polymer precursor exhibits well crystalline structure. XRD examination also indicated that no phases other than rare earth borate are detectable with Eu^{3+} (Tb^{3+}) contents up to 8 mol % after being annealed at 1100 °C. Among these XRD diffraction peaks for the five selected samples match very well with the standard values (JCPDS 16-0277), suggesting the hexagonal phase with vaterite-type structure. For samples prepared in this work, the intensity of XRD peaks is very strong, indicating the good crystalline state of the samples.

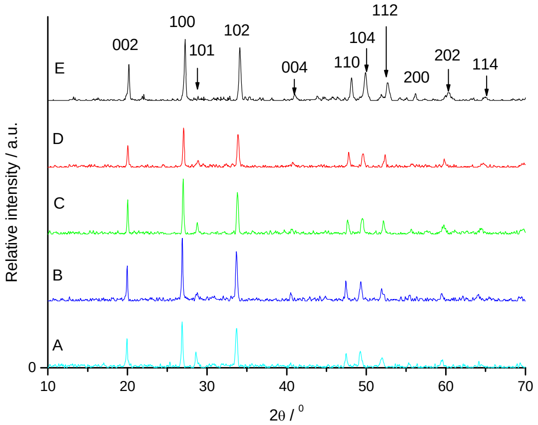

Fig. 1. XRD pattern of submicrometer REBO$_3$: Ln^{3+} phosphors: (A) YBO$_3$: 0.05Eu^{3+}, (B) Y$_{0.5}$Gd$_{0.5}$BO$_3$: 0.05Eu^{3+}, (C) Y$_{0.3}$Gd$_{0.7}$BO$_3$: 0.05Eu^{3+}, (D) GdBO$_3$: 0.05Eu^{3+} and (E) GdBO$_3$: 0.05Tb^{3+}.

We further used the scanning electron microscopy (SEM) to measure the representative submicrometer REBO$_3$: Ln^{3+} derived from assembling multicomponent hybrid precursors (as shown in Figs. 2 and 3), which show the regular microstructure with uniform particle except for a little conglomeration phenomena owing to the high temperature of thermal decomposition. It can be predicted approximately that the REBO$_3$: Ln^{3+} crystal particle sizes are around 100 – 300 nm. Besides, REBO$_3$: Eu^{3+} phosphors present coral-like grain, while REBO$_3$: Tb^{3+} phosphors present the more regular microstructure with good crystal state and uniform particle size. This may be due to the fact that Tb^{3+} and Y^{3+}, Gd^{3+} ions all belong to the heavy rare earth ions while Eu^{3+} not, so the radius of Tb^{3+} and Y^{3+}, Gd^{3+} are similar and Tb^{3+} is easy to substitute Y^{3+}, Gd^{3+}, which can not change the lattice structure of REBO$_3$ host. In this synthesis process, rare earth coordination polymers and organic polymer can be composed to form the interpenetrating network polymeric network structure for both of them possess the similar polymeric structure. The special hybrid precursors may behave as dispersion media, especially as template to have some influence on the control of microstructure or micromorphology of the resulting phosphors. Consequently, this preparation technology connects the synthesis of submicrometer material with the assembly of hybrid material, which can be expected to be a candidate for the synthesis of other luminescent materials based on rare earth oxides.

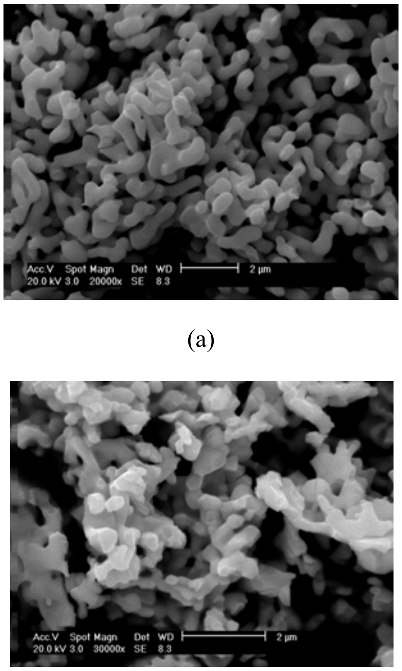

(a)

(b)

Fig. 2. SEM picture of submicrometer submicrometer (A) $Y_{0.5}Gd_{0.5}BO_3$: $0.05Eu^{3+}$, (B) $Y_{0.3}Gd_{0.7}BO_3$: $0.05Eu^{3+}$.

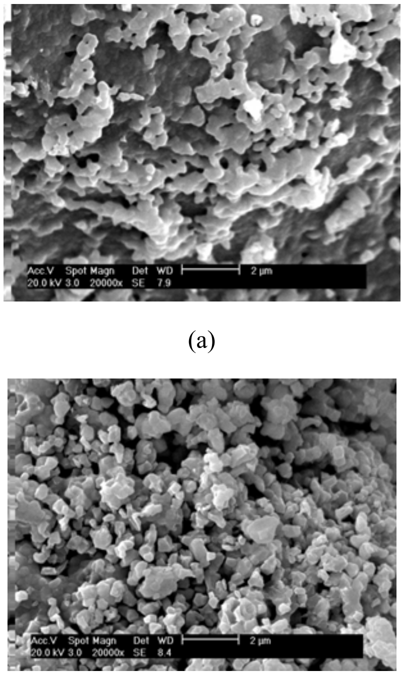

(a)

(b)

Fig. 3. SEM picture of submicrometer submicrometer (A) $GdBO_3$: $0.05Eu^{3+}$ and (B) $GdBO_3$: $0.05Tb^{3+}$.

Figs. 4 present the excitation spectra of $REBO_3$: Eu^{3+} (emission wavelengths of 614 nm). The excitation bands consist of a strong absorption band centered at 222 nm in the short ultraviolet region within the range of 200 nm to 280 nm, while the f-f absorption lines of Eu^{3+} are too weak to be observed clearly in the longer wavelength ultraviolet region of 280 nm to 400 nm. The former is due to the host absorption and spin-allowed $4f^8$-$4f^7 5d$ transitions to form the charge transition state ($O^{2-} \rightarrow Eu^{3+}$), respectively. The strong absorption derive from the vacuum ultraviolet region to about 230 nm is originated from BO_3^{2-} framework and the ultraviolet region of 230 to 280 nm is ascribed to charge transition bands with their exact position being dependent on the crystal field of the lattice [23]. The excitation spectra for $REBO_3$: Tb^{3+} phosphors show the similar features.

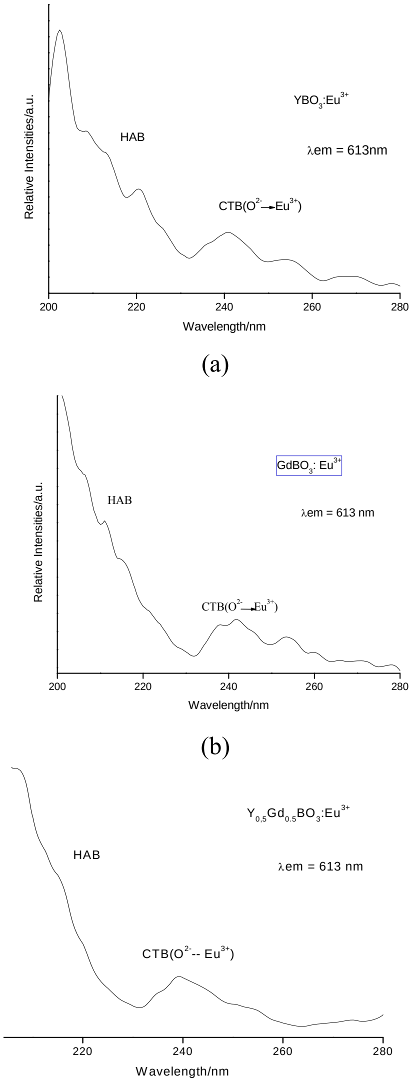

(a)

(b)

(c)

Fig. 4. Excitation spectra of submicrometer $REBO_3$: Eu^{3+} phosphors.

Fig. 5 shows the emission spectra of YBO$_3$ (A) and GdBO$_3$ (B) phosphors doped with different concentrations of Eu^{3+} (for λex = 241 nm), which exhibit the characteristic luminescence originated from the transition between the excited $^5D_0$ level and ^7F_J (J = 1, 2, 3) level of the Eu^{3+} ion, i.e. three peaks at around 591.5 and 610.5 (621) and 651.5 nm, respectively. The predominant red luminescence is from hypersensitive electronic dipole transition $^5D_0 \rightarrow {}^7F_2$ of Eu^{3+} located at 610.5 (621) nm. No emission peak position changes, caused by the doping concentration of Eu^{3+}, were observed in this work. Besides, there exists apparent difference between the YBO$_3$ and GdBO$_3$ phosphors. In the emission spectra of YBO$_3$: Eu^{3+} (Fig. 6(A)), the red emission intensity for electronic transition ($^5D_0 \rightarrow {}^7F_2$) is stronger than orange emission intensity of magnetic transition ($^5D_0 \rightarrow {}^7F_2$), which suggest submicrometer YBO$_3$ host is suitable for the red luminescence and the monochromatism. While for GdBO$_3$: Eu^{3+} (Fig. 6(B)), the red emission intensity for electronic transition ($^5D_0 \rightarrow {}^7F_2$) is close to the orange emission intensity of magnetic transition ($^5D_0 \rightarrow {}^7F_2$), indicating that submicrometer GdBO$_3$ host is unsuitable for the monochromatism. Furthermore, the luminescence intensity obviously increases with increasing doping concentration of Eu^{3+} ions until the quenching effect takes place up to 7 mol %.

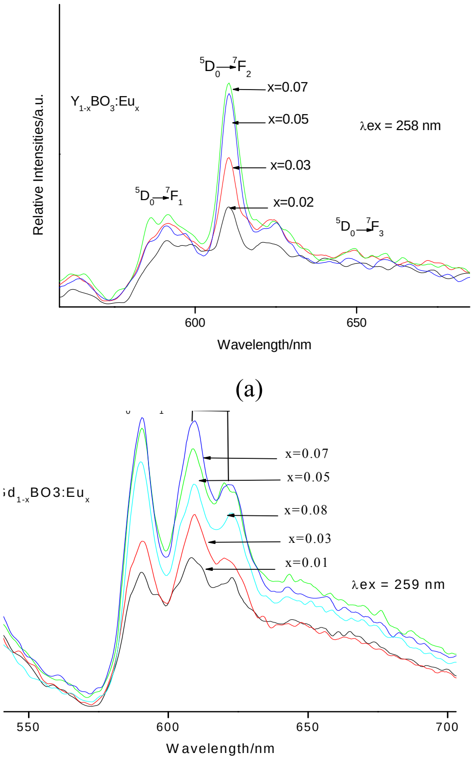

(a)

(b)

Fig. 5. Comparison of emission spectra of REBO$_3$: Ln^{3+} phosphors (A) YBO$_3$: Eu^{3+}, (B) GdBO$_3$: Eu^{3+}.

Fig. 6 shows the emission spectra of Tb^{3+} activated YBO$_3$ (A) and GdBO$_3$ (B) phosphors with different concentrations of Tb^{3+} (for λ_{ex} = 242 nm), which exhibit the characteristic green luminescence originated from the transition between the excited $^5D_4$ level and ^7F_J (J = 6, 5) level of the Tb^{3+} ion, i.e. four peaks at around 489, 542, 592 and 621 nm, respectively. The predominant green color from magnetic dipole transition $^5D_4 \rightarrow {}^7F_5$ of Tb^{3+} located at 542 nm can be explained by taking into account the band ratio β of the $^5D_4 \rightarrow {}^7F_J$ (J = 0-6) transitions which is given by the Judd–Ofelt theory [23, 24]. Furthermore, the luminescence intensity obviously increases with increasing solution concentration of Tb^{3+} ions. Furthermore, the luminescence intensity obviously increases with increasing doping concentration of Tb^{3+} ions and quenching effect takes place up to 7 mol %.

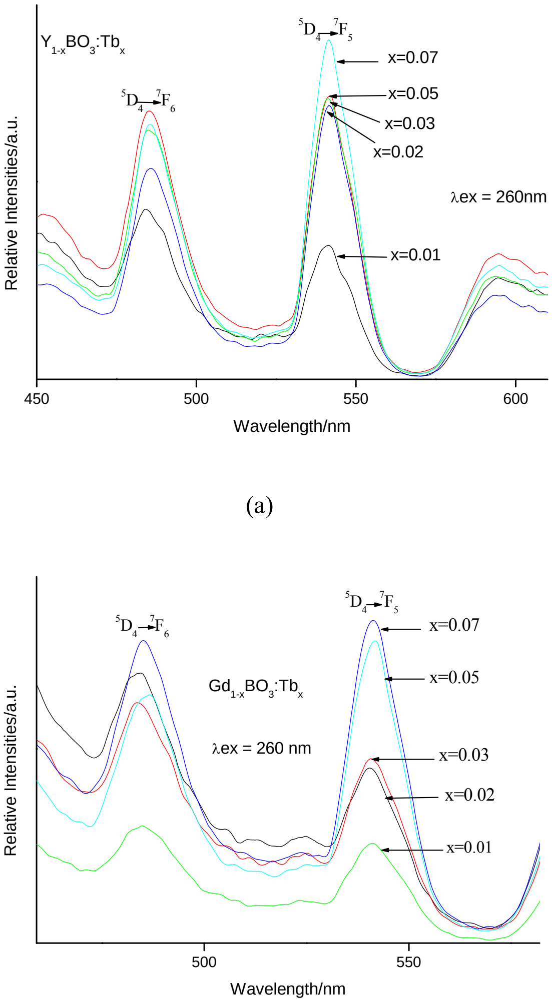

(a)

(b)

Fig. 6. Comparison of emission spectra of REBO$_3$: Ln^{3+} phosphors (A) YBO$_3$: Tb^{3+}, (B) GdBO$_3$: Tb^{3+}.

Fig. 7 shows the emission spectra of $Y_{1-y}Gd_{1y}BO_3$: Eu^{3+}; Tb^{3+} with different molar ratio of Y to Gd, which exhibit that all the spectra have the similar properties. For $Y_{1-y}Gd_{1y}BO_3$: Eu^{3+} (Fig. 7(A)) the different compositions of host have little influence on the emission intensities of Eu^{3+}, the orange emission (592 nm) is strong equivalent to the red one (611, 621 nm) corresponds to the magnetic transition $^5D_0 \rightarrow {}^7F_1$ and electronic transition $^5D_0 \rightarrow {}^7F_2$ can be detected. And the intensity ration of red-to-orange (R / O) is hardly influenced by the value of x in the system of Y_1-Gd_yBO_3: Eu^{3+}. This can be explained that the Y/B ratio is related to many factors, including the site symmetry, charge-to- radius of Ln^{3+} and electro negativity of the next-neighbor element. Similarly, for $Y_{1-y}Gd_{1y}BO_3$: Tb^{3+} (Fig. 7(B)), the different compositions of host have little influence on the emission intensities of Tb^{3+}, the blue emission (489 nm) and the red one (544 nm) are originated from the $^5D_4 \rightarrow {}^7F_6$ and electronic transition $^5D_4 \rightarrow {}^7F_5$ can be observed.

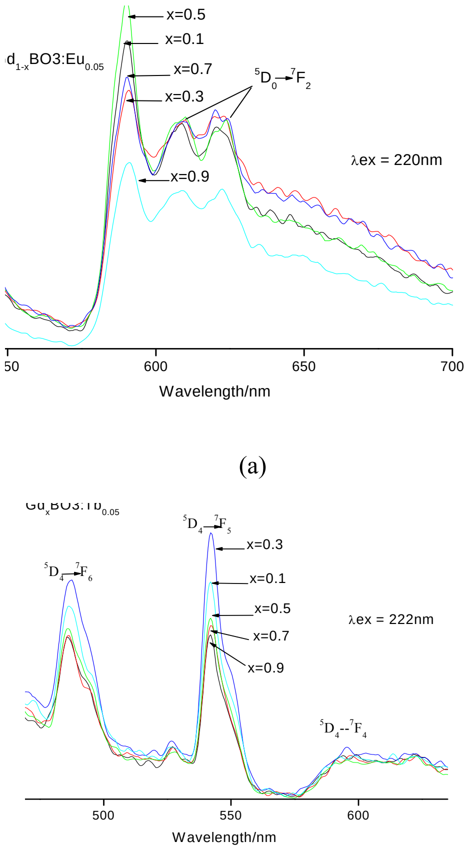

(a)

(b)

Fig. 7. Comparison of emission spectra of $REBO_3$: Ln^{3+} phosphors for different host composition (A) $REBO_3$: Eu^{3+}, (B) $REBO_3$: Tb^{3+}.

4. Conclusion

In summary, we have reported on the matrix-inducing sol-gel synthesis of $REBO_3$: Ln^{3+} (RE = Y, Gd; Ln = Eu, Tb) submicrometer phosphors by in-situ assembling salicylate coordination polymers-PEG precursors at 1100 °C. The particles have the size in the range of 100 – 300 nm and show vaterite-type structure. The submicrometer $REBO_3$: Ln^{3+} (RE = Y, Gd; Ln = Eu, Tb) phosphors exhibit characteristic red-orange luminescence of Eu^{3+} at 592 nm and 611 nm (621 nm) for different host and green emission of Tb^{3+} at 543 nm, which indicates that assembling multicomponent hybrid polymeric precursors is a potential technology for the synthesis of submicrometer phosphors based on rare earth oxides and relevant systems.

Acknowledgement

This work is supported by the Science Development Fund of Tongji University for Excellent Scientists and the National Natural Science Foundation of China (20671072).

References

[1] D. M. Burland, R. D. Miller, C. A. Walsh, Chem. Rev. **94**, 31 (1994).
[2] K. G. Cho, D. Kumar, D. G. Lee, S. L. Jones, P. H. Holloway, R. K. Sinh, Appl. Phys. Lett. **71**, 3335 (1997).
[3] H. X. Zhang, C. H. Kam, Y. Zhou, X. Q. Han, S. Buddhudu, Y. L. Lam, C. Y. Chan, Thin Solid Films **370**, 50 (2000).
[4] Q. Y. Zhang, K. Pita, W. Ye, W. X. Que, Chem. Phys. Lett. **351**, 163 (2002).
[5] C. H. Kim, I. E. Kwon, C. H. Park, Y. J. Hwang, H. S. Bae, B. Y. Yu, C. H. Pyun, G. Y. Hong, J. Alloys Comps. **311**, 33 (2000).
[6] D. Boyer, G. Bertrand, R. Mahiou, J. Lumin. **104**, 229 (2003).
[7] T. Kim, S. Kang, Mater. Res. Bull. **40**, 1945 (2005).
[8] M. Anitha, M. Mohapatra, R. M. Kadam, T. K. Seshagiri, A. K. Tyagi, V. Natarajan, J. Mater. Res. **21**, 1117 (2006).
[9] L. He, Y. H. Wang, Mater. Sci. Forum **1829**, 475-479 (2005).
[10] F. Wen, W. Li, Z. Liu, T. Kim, K. Yoo, S. Shin, J. H. Moon, J. H. Kim, Solid State Commun. **133**, 417 (2005).
[11] J. Zhang, J. Lin, J. Cryst. Growth **271**, 207 (2004).
[12] Y. H. Wang, X. Guo, T. Endo, Y. Murakami, M. Ushirozawa, J. Solid State Chem. **177**, 2242 (2004).
[13] X. C. Jiang, L. D. Sun, C. H. Yan, J. Phys. Chem. B **108**, 3387 (2004).
[14] Z. G. Wei, L. D. Sun, C. S. Liao, X. C. Jiang, C. H. Yan, Y. Tao, X. Y. Hou, X. Ju, J. Appl. Phys. **93**, 9783 (2003).

[15] K. N. Kim, H. K. Jung, H. D. Park, D. Kim, J. Mater. Res. **17**, 907 (2002).
[16] X. G. Wei, L. D. Sun, C. S. Liao, X. C. Jiang, C. H. Yan, J. Mater. Chem. **12**, 3665 (2002).
[17] L. L. Wang, Y. H. Wang, J. Lumin. doi:10.1016/j.jlumin.2006.01.327
[18] K. Y. Jung, E. J. Kim, Y. C. Kang, J. Electrochem. Soc. **151**, H69 (2004).
[19] C. K. Lin, M. L. Pang, M. Yu, J. Lin, J. Lumin. **114**, 299 (2005).
[20] Y. H. Wang, J. C. Zhang, X. Guo, Electrochem. Solid State Lett. **9**, H26 (2006).
[21] Z. H. Li, J. H. Zeng, C. Chen, Y. D. Li, J. Cryst. Growth **286**, 487 (2006).
[22] D. J. Robbins, B. Cockayne, B. Leut, J. L. Glasper, Solid State Commun. **20**, 673 (1976).
[23] B. R. Judd, Phys. Rev. **127**, 750 (1962).
[24] G. S. Ofelt, J. Chem. Phys. **37**, 511 (1962).

---

*Corresponding author: byan@tongji.edu.cn